

Numerical Simulation - a Design Tool for Electro Hydraulic Servo Systems

Popescu T.C.¹, Vasiliu D.² and Vasiliu N.²

¹*National Institute for Optoelectronics, INOE 2000-IHP Bucharest,*

²*University „Politehnica” of Bucharest
Romania*

1. Introduction

Electro hydraulic servo systems are complex technical entities that involve both phenomena of fluid mechanics, and phenomena specific to control processes with feedback. Due to the complexity of these interactions, the optimal design goal is achieved by an iterative process, using some dedicated software. To obtain the required performance the use of mathematical modeling and numerical simulation of these systems is always very effective. In any optimal synthesis process of an electro hydraulic control systems, the analysis of the stability is an important stage. Several methods are used to provide a good stability for such type of systems: the increase of the dead band of the control valves, the use of some additional feedback, the decrease of the flow gain of the control valve around the hydraulic null point etc.

Numerical simulation of the dynamic systems allows gathering of necessary information about their behaviour based on a mathematical models that describe those systems. Obtaining of mathematical models as close as possible to the physical phenomena that are to be reproduced or improved is helpful in making decisions for optimization. The most recent tendencies in this field regard novel concepts, such as co-simulation and real time simulation.

This chapter presents two different examples of developing a numerical co-simulation environment, based on two software packages: AMESim (LMS IMAGINE SA, 2009) and LabVIEW (National Instruments, 2009). The most important parameters investigated are the following:

- a. **the influence of the variable area gradient** of an electrohydraulic flow amplifier on the stability reserves of a electro hydraulic servomechanism (a. Ion Guta et al., 2010);
- b. **a hybrid solution of modeling / simulation** of a hydrostatic transmission with mixed control (b. Ion Guta et al., 2010).

By means of AMESim software a model of an electrohydraulic servomechanism was developed, while analysis of data collected as a result of simulations in AMESim was performed by means of virtual instrumentation, using LabVIEW software. The real time use of these two simulation / programming environments can lead to the development of advanced modeling / simulation networks of complex fluid systems controlled by digital hardware, useful for optimal system design.

2. The stability of electrohydraulic servomechanisms developed with electrohydraulic amplifiers of variable area gradient

2.1 Mathematical modeling of electrohydraulic servomechanism

Mathematical model of an electrohydraulic servomechanism with position response comprises the following equations (Vasiliu & Vasiliu, 2005): Equation of slide valve displacement; Equation of position transducer; Equation of electronic comparator; Continuity equation of subsystem directional control valve-hydraulic cylinder; Equation of current generator of proportional compensator; Motion equation of hydraulic cylinder's piston; Characteristic of directional control valve with variable area gradient.

The power stage of this valve is represented by an adjustment directional control valve, with 4 ways and 3 positions, with closed critical center. For a directional control valve with variable area gradient, fig.1, we hold:

Geometrical characteristics of unit sleeve – slide valve: $D=2R$ – diameter of main slide valve; $d = 2r$ – diameter of circular distribution window; a – width of rectangular distribution windows; b – length of rectangular distribution windows.

The following notations are introduced:

$$\begin{aligned} c_{x1} &= b \\ c_{y1} &= R \cdot \arcsin(0.5 \cdot a / R) \\ c_{x2} &= b + \sqrt{r^2 - (c_{y1} \cdot r / c_{y2})^2} \\ c_{y2} &= R \cdot \arcsin(r / R) \end{aligned} \quad f(x) = \begin{cases} c_{y1}, & x \in (0, b) \\ \frac{c_{y2}}{r} \cdot \sqrt{r^2 - x^2}, & x \in (b, c_{x2}) \end{cases} \quad (1)$$

Law of variation of drainage area, depending on stroke of slide valve, is:

$$A(x) = \begin{cases} 2 \cdot c_{y1} \cdot x, & x \in (0, b) \\ 2 \cdot \frac{c_{y2}}{r} \cdot \int_b^{c_{x2}} \sqrt{r^2 - x^2} dx, & x \in (b, c_{x2}) \end{cases} \quad (2)$$

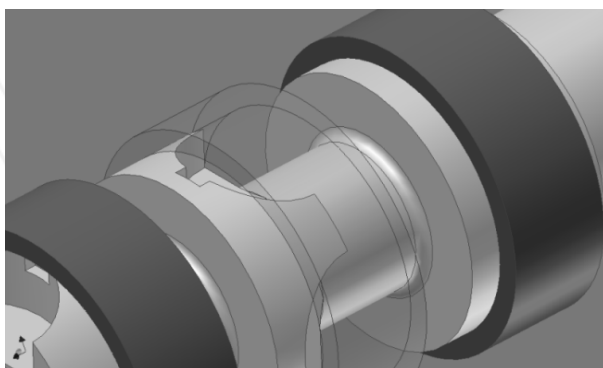


Fig. 1. Slide valve of directional control valve with variable area gradient

Slide valve of directional control valve with variable area gradient (Bosch Rexroth Group) is shown in fig.1, while variation of area of directional control valve's holes – in fig. 2. Zone I, fig.

2, is the area where drainage takes place through rectangular windows (around null), while zone II corresponds to drainage through the two distribution windows, respectively with rectangular area and quasi-elliptical area, resulted from intersection of two cylindrical bodies.

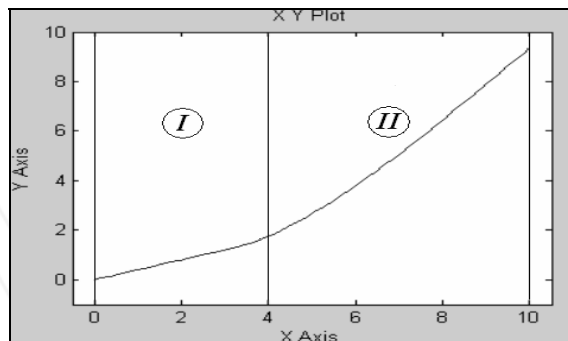


Fig. 2. Variation of area of holes, depending on relative displacement between slide valve and sleeve

Characteristics of stationary mode of directional control valve is:

$$Q = c_d \cdot A(x) \cdot \sqrt{\frac{p_s}{\rho} \left(1 - \frac{x}{|x|} \cdot \frac{p}{p_s} \right)} \quad (3)$$

For the two operation zones, flow can be calculated with the following relations:

$$Q(x) = \begin{cases} c_d \cdot 2 \cdot c_{y1} \cdot x \cdot \sqrt{\frac{p_s - p}{\rho}}, & x \in (0, b) \\ c_d \cdot 2 \cdot \left(c_{y1} b + \frac{c_{y2}}{r} \cdot \int_b^{c_{x2}} \sqrt{r^2 - x^2} dx \right) \cdot \sqrt{\frac{p_s - p}{\rho}}, & x \in (b, c_{x2}) \end{cases} \quad (4)$$

Flow amplification factor depends on operation zone:

$$K_{Qx} = \frac{\partial Q}{\partial x} = \begin{cases} c_d \cdot 2 \cdot c_{y1} \cdot \sqrt{\frac{p_s - p}{\rho}}, & x \in (0, b) \\ c_d \cdot 2 \cdot \frac{c_{y2}}{r} \cdot \sqrt{r^2 - x^2} \cdot \sqrt{\frac{p_s - p}{\rho}}, & x \in (b, c_{x2}) \end{cases} \quad (5)$$

Coefficient flow-pressure can be calculated with the following relations:

$$K_{QP} = \frac{\partial Q}{\partial P} = \begin{cases} \frac{c_d \cdot 2 \cdot c_{y1} \cdot x}{\sqrt{\rho(p_s - p)}}, & x \in (0, b) \\ \frac{c_d \cdot A(x)}{\sqrt{\rho(p_s - p)}}, & x \in (b, c_{x2}) \end{cases} \quad (6)$$

$$K_P = K_{QP} + K_1$$

Equation of slide valve displacement:

Flow control valve can be considered a delay factor of first rank:

$$\frac{x(s)}{i(s)} = \frac{K_{xi}}{T_s s + 1} \quad (7)$$

Or

$$T_s s x(s) + x(s) = K_{xi} i(s) \quad (8)$$

The following differential equation results:

$$T_s \frac{dx}{dt} + x = K_{xi} i(t) \quad (9)$$

T_s - time constant of directional control valve.

Equation of position transducer:

$$U_T = K_T y \quad (10)$$

K_T - is the constant of transducer, [V/m]

y - displacement of piston of hydraulic cylinder

Equation of electronic comparator:

$$\varepsilon = U_0 - U_T \quad (11)$$

ε - adjustment error.

Equation of current generator of proportional compensator:

$$i = K_{ie} \varepsilon \quad (12)$$

K_{ie} [A/V] - conversion factor

Continuity equation of subsystem directional control valve-hydraulic cylinder:

$$Q = A_p \dot{y} + K_i P + \frac{A_p^2}{R_h} \dot{P} \quad (13)$$

A_p - piston area;

K_i - coefficient of drainage between hydraulic cylinder's chambers;

R_h - hydraulic rigidity of double-effect hydraulic cylinder

Motion equation of hydraulic cylinder's piston

Pressure force F_p must overcome elastic force F_e , dissipation factor (the damper) F_a , friction force, F_f and inertial force, so:

$$m_c \ddot{y} = F_p - F_a - F_e - F_f \quad (14)$$

Where,

$$F_p = A_p P \quad (15)$$

$$F_a = K_f \cdot v \quad (16)$$

$$F_e = 2(K_{e1} + K_{e2})(y + y_{0e}) = 2K_e(y + y_{0e}) \quad (17)$$

For friction force between piston and cylinder a static component F_{fs} and a viscous one F_{fv} are both considered:

$$F_{fs} = F_{fs0} \text{sign} \dot{y} \quad (18)$$

$$F_{fv} = K_{fv} \dot{y} \quad (19)$$

2.2 Numerical co-simulation. Identification of a linearized model

Identification aims at determining static and dynamic characteristics of processes. By identification it is understood the procedure of determining a system based on one input and one output, in case of SISO systems (single input - single output), so that it is equivalent, in a certain way, to the tested system.

Identification of parameters of mathematical model based on experimental data implies four stages: acquisition of input/output data; choosing structure of the model; estimation of parameters of the model; validation of the identified model (validation of structure and value of parameters) (Calinoiu et al., 1998).

For the analyzed case we used identification procedures of ARX models (functions which use the method of least squares) in LabVIEW. ARX models have the following structure:

$$A(q)y(t) = B(q)u(t-nk) + e(t) \quad (20)$$

The identified models were the basic elements of the study, with their support Bode diagrams and transfer loci of the analyzed process are drawn.

Study of stability of automatic electro hydraulic systems can be performed based on algebraic criterion Routh - Hurwitz, which has only one condition for stability or on Nyquist criterion, which allows in addition analysis of stability reserves (Catana et al., 1996). Transfer locus of open circuit system looks like in fig. 3. Necessary and sufficient condition for closed circuit system to be stable is that the hodograph of linear model not surround the critical point $(-1, j0)$ in the complex plane when the frequency belongs to the interval $(0, \infty)$. Stability reserve of the system can be evaluated by two characteristic sizes: the amplitude edge (stability reserve in modulus) and the phase edge (stability reserve in phase).

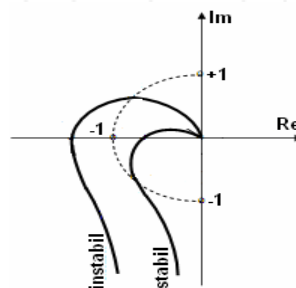


Fig. 3. Transfer locus of servo mechanism

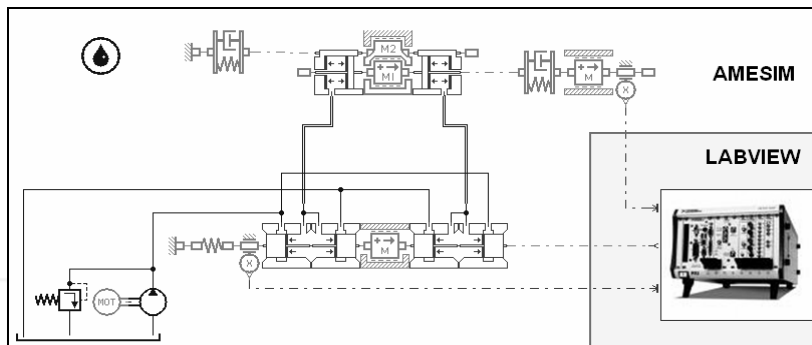


Fig. 4. Co-simulation network of analyzed servo mechanism

In fig.4 can be noticed the co-simulation network of the analyzed system. Numerical model developed in the AMESim allows analysis of behaviour over time of the examined system. Based on response to various excitation signals can be identified, by means of the model developed in LabVIEW, mathematical linearized model of the system, based on which can be performed system stability analysis.

To study system stability the transfer locus of servo mechanism was used by means of Nyquist outline analysis. The exchange of information between submodel of dynamic system of servo mechanism, developed in AMESim and compensator submodel, implemented in LabVIEW, can be achieved by shared access to a specific memory area if the networks run on the same system or by a communication channel TCP / IP if the networks run on two different systems.

Architecture of the process is *master / slave* type, the integration step is determined by the master system.

Co-simulation network, fig.4, is made of: the group of oil supply under constant pressure (constant speed electric motor, volumetric pump, normally closed valve); electro-hydraulic directional control valve with variable area gradient; linear hydraulic motor with double effect and double rod; inertial load; displacement transducer for slide valve of distributor; displacement transducer for the hydraulic cylinder rod; control software interface, analysis and interpretation of data, developed in LabVIEW.

The calculations were performed for these data: $m_{load} = 100 \text{ Kg}$, $p_{supply} = 160 \text{ bar}$, $cylinder_stroke = 300 \text{ mm}$, $d_{cylinder} = 26 \text{ mm}$, $d_{rod} = 12 \text{ mm}$, $anchor \text{ rigidity} = 2.1 \cdot 10^7 \text{ N/m}$, $damping \text{ coefficient} = 4000 \text{ Ns/m}$.

The model was excited with signals type *white noise*. To establish the transfer locus, the model was examined in open loop, after drawing features we also developed chart of response over time to step closed-loop signals. ARX models identified were determined for each operating mode. Results of co-simulation are presented in figures 5, 6, 7, 8 and 9.

Discret mathematical models identified for open-loop system with: (a) - directional control valve without variable area gradient, (b)- directional control valve with variable area gradient:

$$(1 - 2.9719z^{-1} + 2.9479z^{-2} - 0.976z^{-3}) y(k) = (-2.3882E-6 + 1.6886E-6z^{-1} + 3.2132E-5z^{-2}) u(k) + e(k) \quad (a)$$

$$(1 - 2.981z^{-1} + 2.9668z^{-2} - 0.9858z^{-3}) y(k) = (-6.9855E-7 + 5.3387E-7z^{-1} + 1.8398E-5z^{-2}) u(k) + e(k) \quad (b)$$

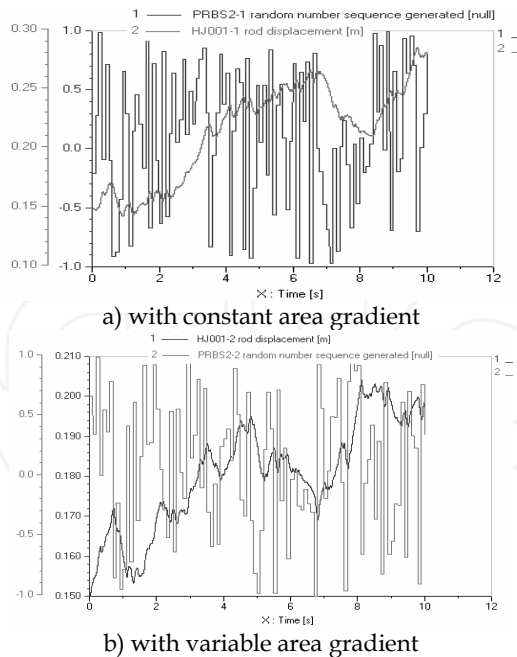


Fig. 5. Response over time of the servo mechanism to control signal of type white noise

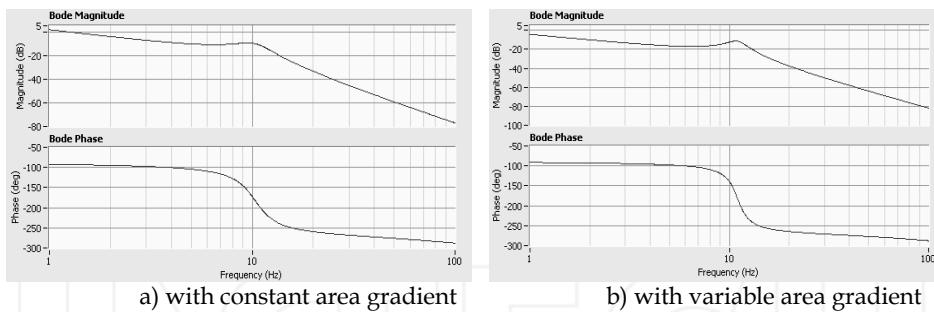


Fig. 6. Bode diagram of the servo mechanism in open loop

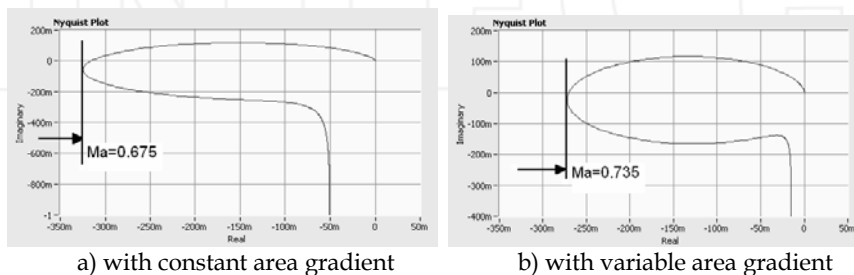
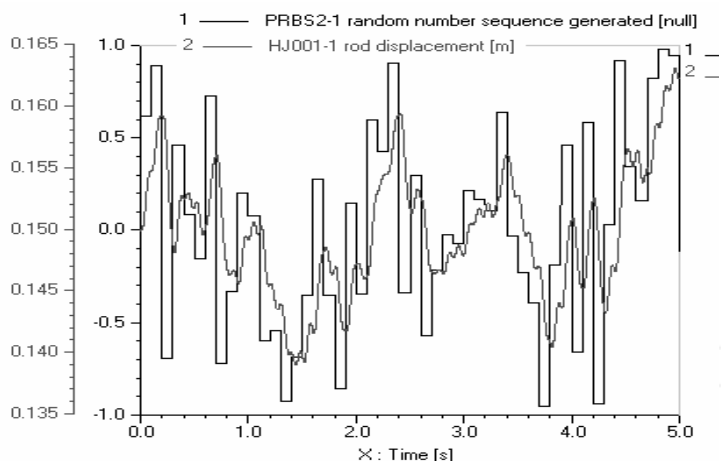
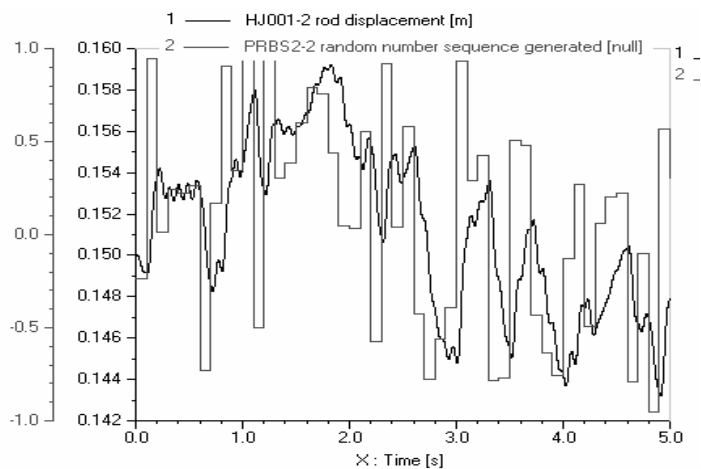


Fig. 7. Hodograph of open-loop system

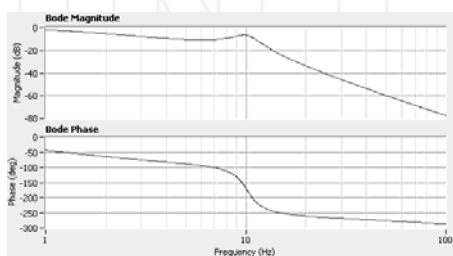


a) with constant area gradient

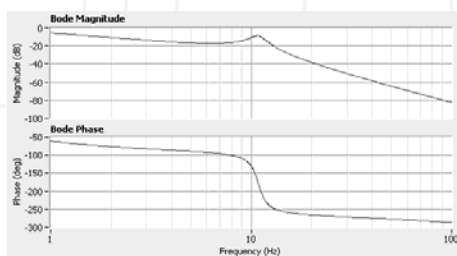


b) with variable area gradient

Fig. 8. Response over time of system in loop of response to control signal of type white noise



a) with constant area gradient



b) with variable area gradient

Fig. 9. Bode diagram of the servo mechanism in closed loop

Discret mathematical models identified for closed-loop system with: (a) – directional control valve without variable area gradient, (b)- directional control valve with variable area gradient:

$$(1 - 2.9727z^{-1} + 2.9495z^{-2} - 0.9768z^{-3}) y(k) = (-1.8146E-6 + 1.2474E-6z^{-1} + 3.0294E-5z^{-2}) u(k) + e(k) \quad (a)$$

$$(1 - 2.9819z^{-1} + 2.9685z^{-2} - 0.9866z^{-3}) y(k) = (-5.7764E-7 + 5.2905E-7z^{-1} + 1.742E-5z^{-2}) u(k) + e(k) \quad (b)$$

3. Optimization of hydrostatic transmissions by means of virtual instrumentation technique

3.1 Problem formulation

The analyzed hydrostatic transmission, of mixed adjustment, with single consumer of type adjustable rotary volumetric motor, according to the basic model in fig.10, includes:

- **in its primary sector:** a MOOG servopump, place 1, with radial pistons and integrated electronics, with three loops of adjustment, that is in flow, in pressure, in flow and pressure, with capacity of 32 cm³/rev, rotary speed of 1450 rev/min, control voltage of 0...10V, flow of 0...46 l/min; an electric motor for servopump actuation, of constant rotary speed, place 2; a pressure limiting valve, place 3; a flow transducer, place 4; and a pressure transducer, place 5.
- **in its secondary sector:** a BOSCH servo motor type EP2, place 7, with axial pistons, tilted block and integrated electronics, with minimum capacity of 7 cm³/rev at control voltage of 200 mA and maximum capacity of 28 cm³/rev at control voltage of 800 mA, at supply voltage of 24Vd.c.; a torque transducer place 8; a speed transducer, place 9; an axial piston pump, with tilted block and fixed capacity place 10, to simulate the load of hydraulic servo motor; two pressure transducers, place 11 and place 13; four way-valves, place 12, fitted on suction / repression side of load pump; a pressure adjustment valve, with electric control, place 14, for adjusting load of hydraulic servo motor.
- **a PXI-NATIONAL INSTRUMENTS block**, place 6, which provides a virtual interface of the adjustment process of capacity of the adjustable volumetric machines (LabVIEW / PXI).

For this hydrostatic transmission we have developed a physical laboratory model, according to fig.11 and fig.12; a numerical simulation network in AMESim, according to fig.13; a virtual interface for the adjustment model of transmission, according to fig.14 and a web interface for the adjustment model of transmission, according to fig.15.

By means of the adjustment model of hydrostatic transmission with mixed adjustment the following items were highlighted:

- **by means of co-simulation AMESim-LabVIEW:** demonstration, on the physical laboratory model, of primary (pump), secondary (motor) and mixed (pump and motor) adjustments, specific to hydrostatic transmissions (Popescu et al., 2010); demonstration, on the physical laboratory model, of the advantages, in terms of energy, of hydrostatic transmissions with adjustable pumps in their primary sector over those with fixed pumps in their primary sector (b. Drumea et al., 2010).
- **by means of simulation models in AMESim:** optimization of the adjustment model of a hydrostatic transmission with mixed adjustment in order to reduce variation of the rotary speed of volumetric motor within its secondary sector, in accordance with variation of its load.

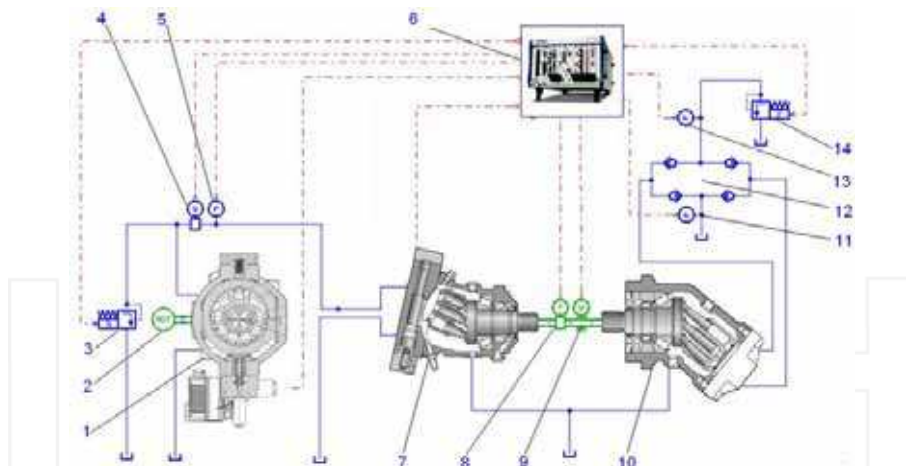


Fig. 10. Basic model of a hydrostatic transmission with mixed adjustment



Fig. 11. MOOG servopump, type RKP-D, within the primary sector



Fig. 12. Bosch servo motor, type EP2, within the secondary sector

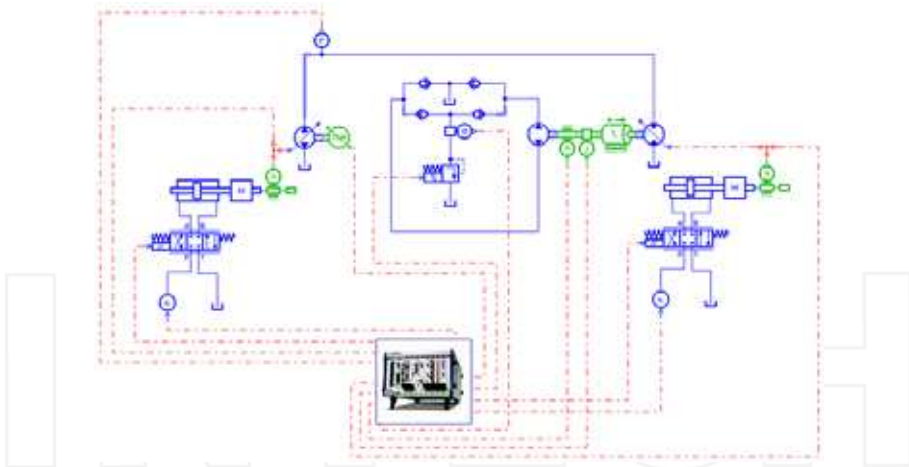


Fig. 13. Simulation network in AMESim of a hydrostatic transmission with mixed adjustment

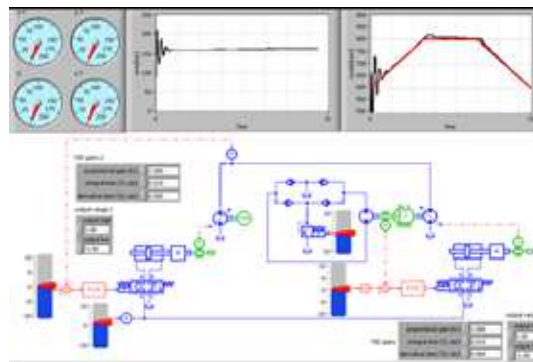


Fig. 14. Virtual interface of the adjustment model (LabVIEW / PXI)

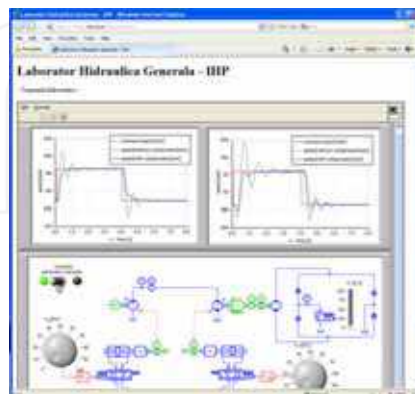


Fig. 15. Web interface of the adjustment model (LabVIEW / PXI)

3.2 Demonstration of adjustment of capacity at adjustable volumetric machines

We have traced the response of the adjustment system of transmission, that actuates upon the servomechanism which adjusts the capacity of the pump within the primary sector or upon the servomechanism which adjusts the capacity of the motor within the secondary sector, to rotational speed step type signal imposed to the volumetric motor within the secondary sector. Within the adjustment model we have preset the rotational speed threshold of 320 r.p.m, below which the adjustment of transmission is performed upon the pump (primary adjustment) and above which the adjustment of transmission is performed upon the motor (secondary adjustment).

Dynamic characteristics of the system were raised, which highlight:

- the influence of a rotational speed step type signal of 312 rpm imposed to the hydraulic motor within the secondary sector, upon the adjustment drive of capacity of the adjustable pump, with and without error compensation, according to fig.16;
- the influence of a rotational speed step type signal of 410 rpm imposed to the hydraulic motor within the secondary sector, upon the adjustment drive of capacity of the adjustable pump, with and without error compensation, according to fig.17;
- the influence of rotational speed step type mixed signals of 308 rpm, respectively 408 rpm, imposed to the adjustable hydraulic motor within the secondary sector, upon the adjustment drive of capacity of the adjustable pump, respectively of the adjustable motor, with and without error compensation, according to fig.18.

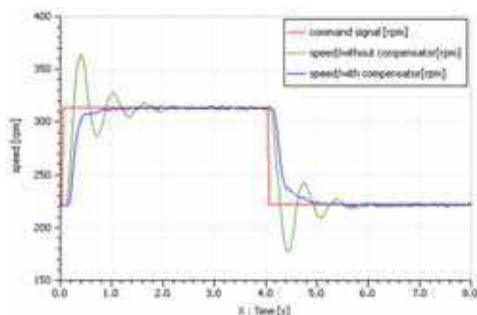


Fig. 16. Response of the adjustment system of rotational speed of hydraulic motor to step type excitation signal – pump capacity drive

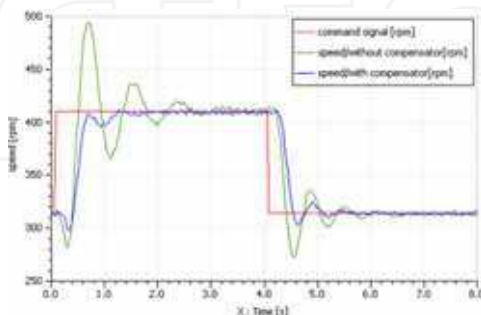


Fig. 17. Response of the adjustment system of rotational speed of hydraulic motor to step type excitation signal – motor capacity drive

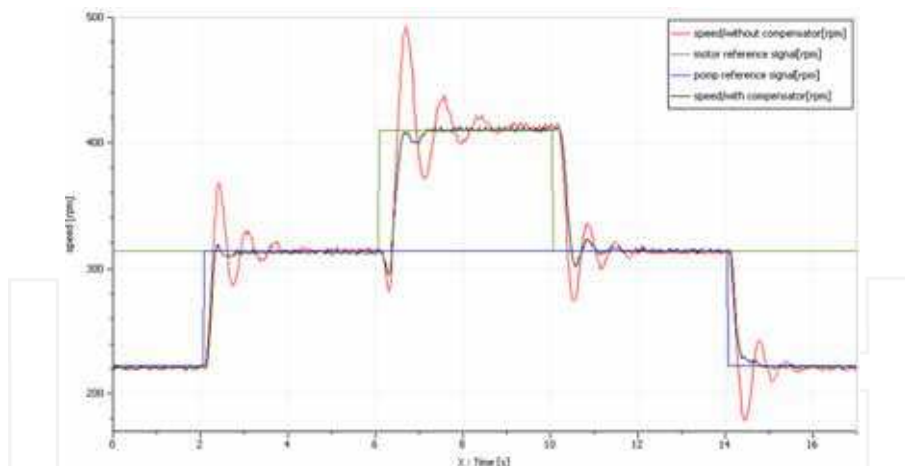


Fig. 18. Response of the adjustment system of rotational speed of hydraulic motor to mixed step type excitation signal – pump and motor capacity drive

3.3 Numerical simulation of radial piston pump MOOG type RKP-D

Simulation model developed for the analysis of volumetric pump in fig.19, is shown in fig.20 (a. Drumea et al., 2010). It includes: the hydraulic servomechanism for prescribing the position of the adjustment ring; a module for calculating the relative position of small pistons as against to their angular position and the ordered eccentricity; the two small radial pistons of the pump; the distribution unit, controlled by the angular position of small pistons and the geometrical characteristics of the distribution flange.

By means of the modeling network developed, dynamic characteristics of the servo motor that adjusts capacity of the analyzed radial piston pump were determined, figures 5 and 6. The model was excited with control signals (prescribing of eccentricity of the flow adjustment / control ring), triangular, sinusoidal and rectangular signals, of various amplitudes and frequencies. Obtained results are compared, simulated and experimentally shown. Simulation model has been "tuned" as a result of the comparative analysis between simulated and experimental response for a better accuracy of results (Popescu et al., 2010).

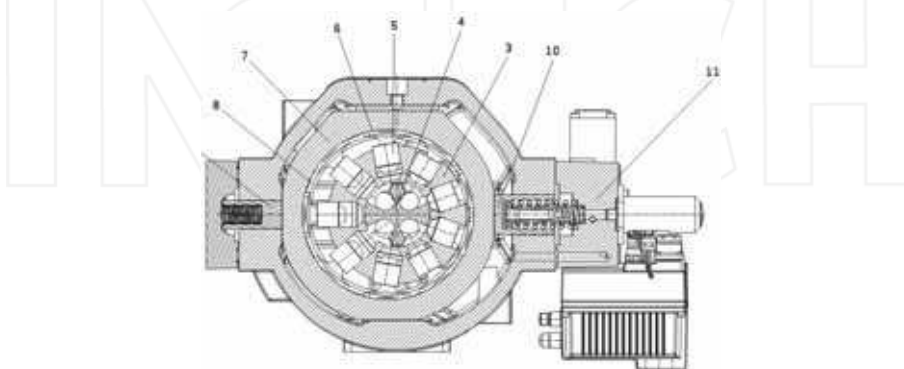


Fig. 19. Servo pump MOOG type RKP-D; cross-section

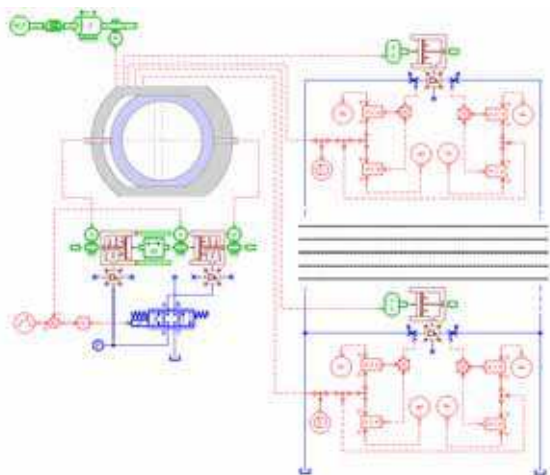


Fig. 20. Servo pump MOOG type RKP -D; numerical simulation model

In figures 21 and 22 curve 1 represents the control signal, curve 2 - response of servomechanism that adjusts capacity, obtained through numerical simulation, and curve 3 - response of servomechanism that adjusts capacity, obtained on an experimental basis.

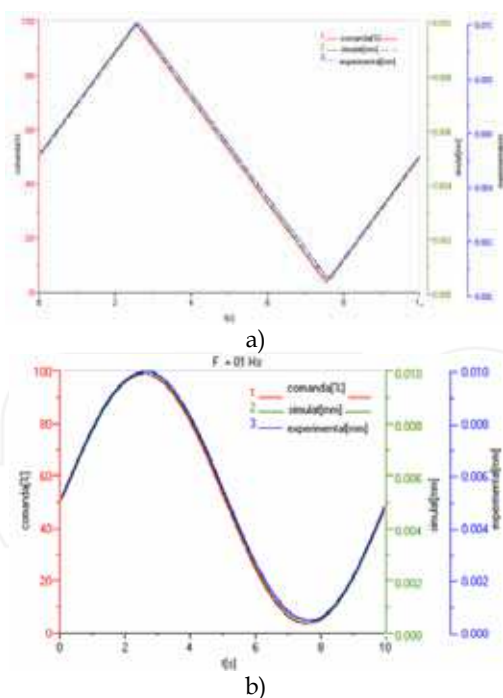


Fig. 21. Response of the adjustment servomechanism to control triangular, (a) and sinusoidal, (b) signals ($f=0.1$ Hz)

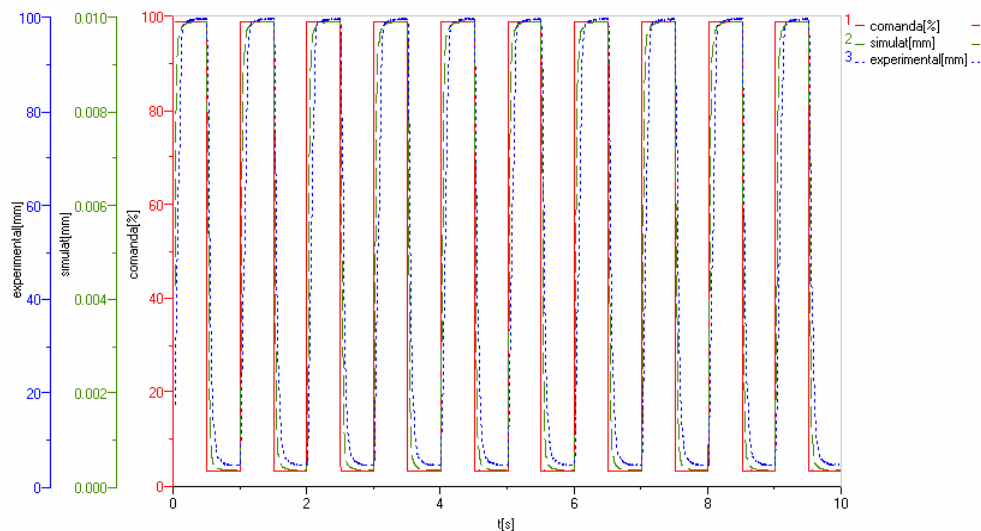


Fig. 22. Response of the adjustment servomechanism to a control rectangular signal ($f=1$ Hz)

3.4 Demonstration of advantages in terms of energy of hydrostatic transmissions with adjustable pumps in their primary sector

Two variants of adjusting the flow within the primary sector of a hydrostatic transmission were tested in comparison, according to fig.23.

- variant (a), where capacity of the pump within the primary sector is set, while flow adjustment is performed by means of an adjustable throttle (Popescu et al., 2009). In this case, the extra flow is discharged at the tank through a normally closed pressure valve;
- variant (b), where in the primary sector a hydraulic servopump with adjustable capacity is used.

In both variants, tests were performed for a constant load of 20 Nm at the shaft of hydraulic motor within the secondary sector of transmission.

After calibrating the adjustment model of mixed adjustment transmission, process carried out by means of the numerical simulation network, the motor within the secondary sector was set on maximum capacity and the two flow adjustments systems for the pump in the primary sector were analyzed comparatively (b. Drumea et al., 2010). Tests were performed for a 20 Nm load at the shaft of the motor within secondary sector of transmission.

Experimentally, systems were excited cyclically, with or without energy efficiency, with step-type control signals of rotational speed (500 rpm), fig.24, and ramp-type signals, fig.25. We recorded evolution over time of rotational speed of the hydraulic motor shaft, fig.24 (a), fig.25 (a) and pressures within primary hydraulic circuit, fig.24 (b), fig.25 (b).

The two systems for adjusting the flow within the primary sector of transmission have been excited with a control signal of the speed of hydraulic motor within the secondary sector, corresponding to a specific preset profile.

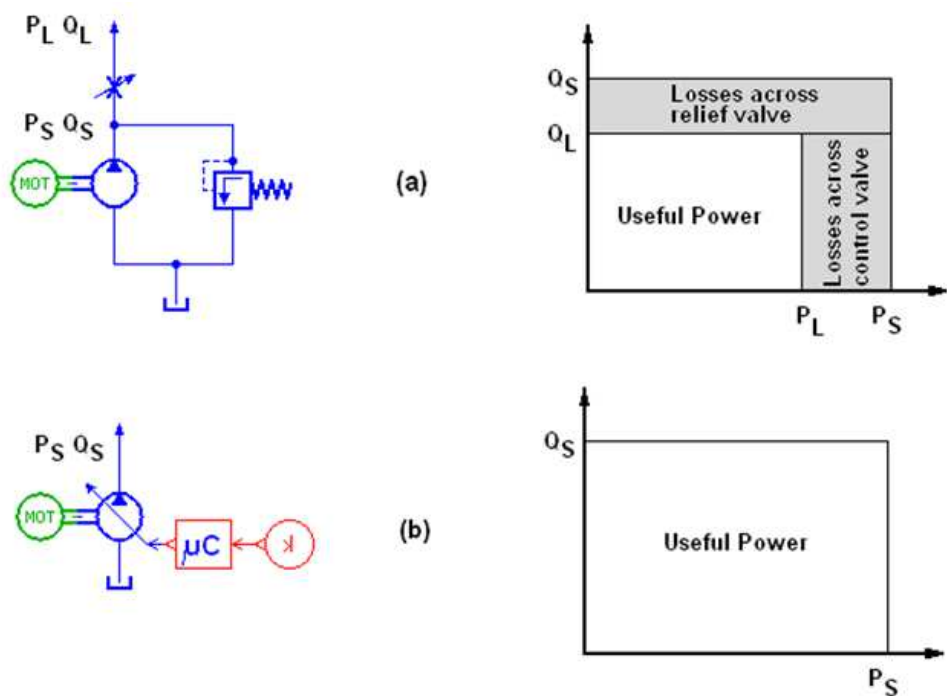


Fig. 23. Variants of adjusting the flow within the primary sector of a hydrostatic transmission

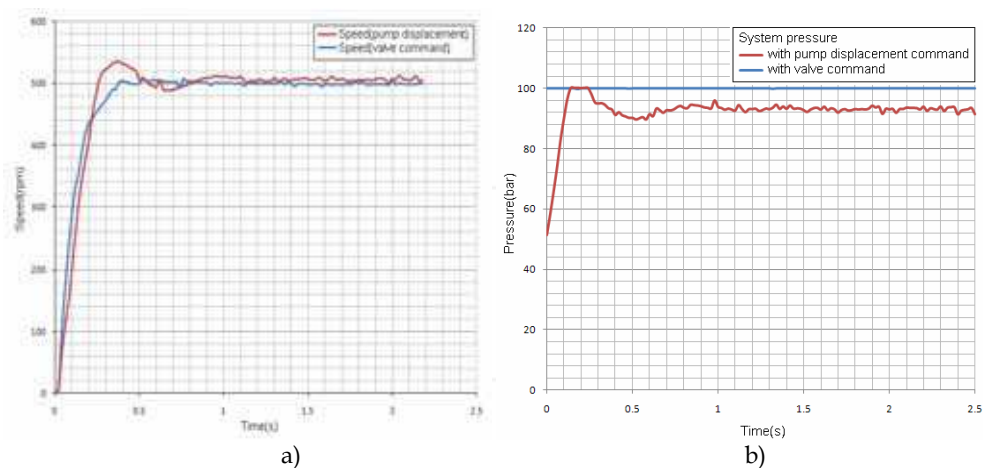


Fig. 24. a) Variation of rotational speed of hydraulic motor within secondary sector to a step type excitation signal of flow adjustment systems within the primary sector, b) Variation of pressure along the primary circuit to a step type excitation signal of flow adjustment systems within the primary sector

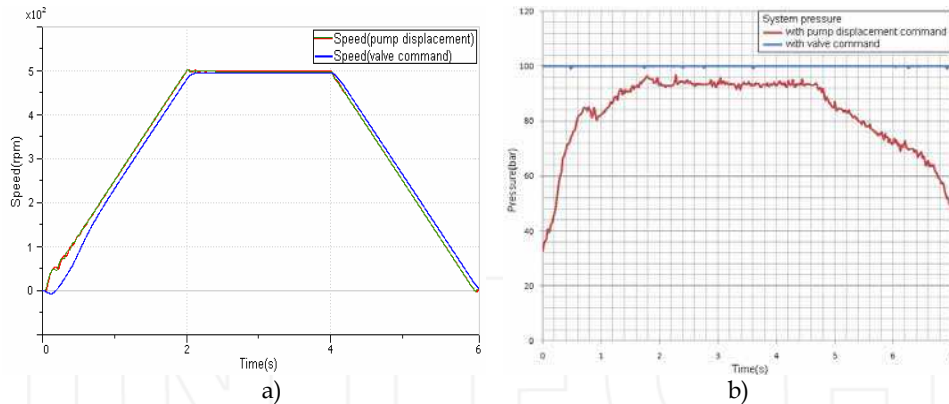


Fig. 25. a) Variation of rotational speed of hydraulic motor within the secondary sector to a ramp type excitation signal of flow adjustment systems within the primary sector, b) Variation of pressure along the primary circuit to a ramp type excitation signal of flow adjustment systems within the primary sector

We have recorded the pressures within the circuit, fig.26 (blue- variation of rotational speed of hydraulic motor; brown- variation of the supply voltage of hydraulic motor in an energy-efficient system; red- variation of the supply voltage of hydraulic motor in an energy-inefficient system).

In fig.27, after calculation of hydraulic power used by the pump within the primary sector ($P=Q \cdot p$), we have traced evolution over time of this power for the two flow adjustment systems, without (brown) and with (blue) energy efficiency.

The obtained data were integrated numerically in order to result the evolution of the consumed energy, fig.28 (brown- energy-inefficient system, blue- energy-efficient system). Area of the surface defined by the two curves represents the energy savings.

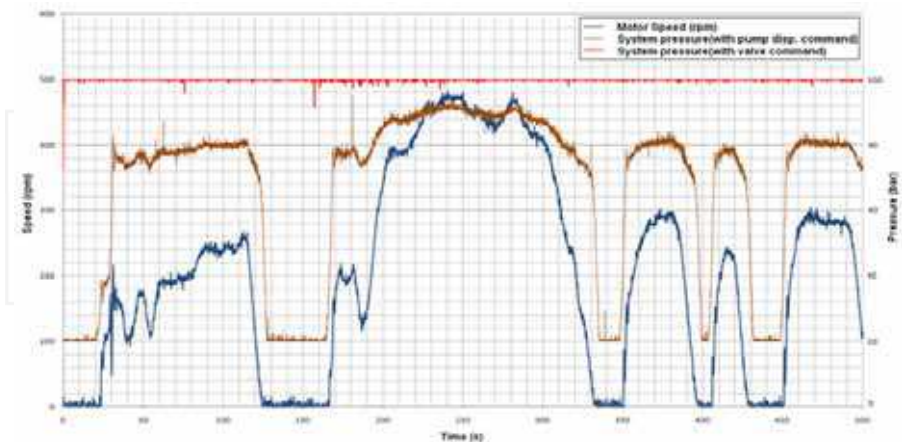


Fig. 26. Variation of pressure along the primary circuit of hydraulic transmission, at control signal with preset profile for rotational speed of the motor within the secondary sector

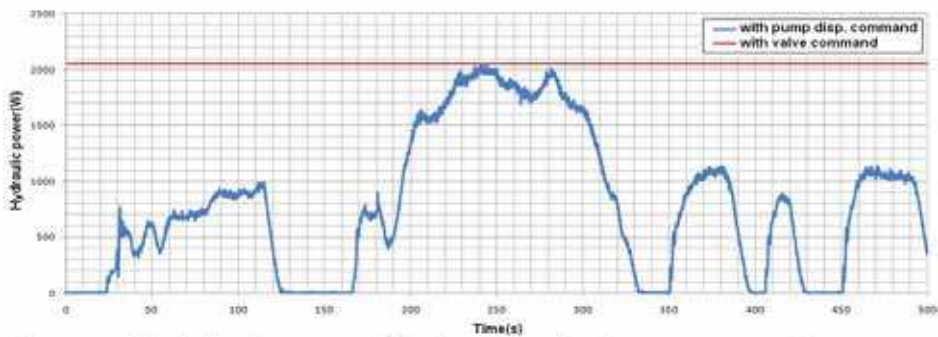


Fig. 27. Variation of the hydraulic power used by the pump within the primary sector of transmission, at control signal with preset profile for rotational speed of the motor within the secondary sector

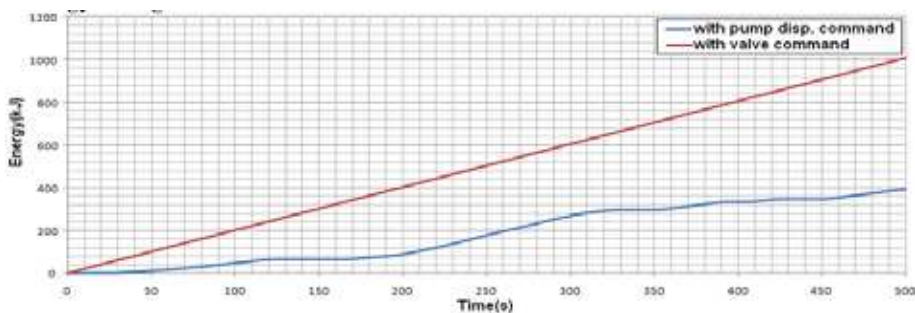


Fig. 28. Variation of energy used by the pump within the primary sector of transmission, at control signal with preset profile for rotational speed of the motor within the secondary sector

3.5 Optimization of the adjustment model of a hydraulic transmission with secondary adjustment

We aimed to optimize the adjustment model of a hydraulic transmission with secondary adjustment, derived from the hydraulic transmission with mixed adjustment. Optimization is performed in view of two goals: to reduce the variation range of rotational speed of the motor within the secondary sector, caused by variation of its load, and to reduce the extra flow discharged through the valve of the pump within the primary sector of transmission.

A pre-step in optimizing the adjustment model of hydrostatic transmission is represented by optimization of the simulation model in AMESim of transmission. In order to achieve this, three variants of simulation models were developed:

- **variant (a)**, according to fig.29: hydraulic transmission with secondary adjustment, with fixed pump and variable motor, with compensator type P (proportional) in the adjustment loop of rotational speed;
- **variant (b)**, according to fig.30: hydraulic transmission with secondary adjustment, with fixed pump and variable motor, with compensator type PID (proportional, integrative, derivative) in the adjustment loop of rotational speed;

- **variant (c)**, according to fig.31: hydraulic transmission with secondary adjustment, with adjustable pump equipped with pressure regulator and variable motor, with compensator type P (proportional) in the adjustment loop of rotational speed.

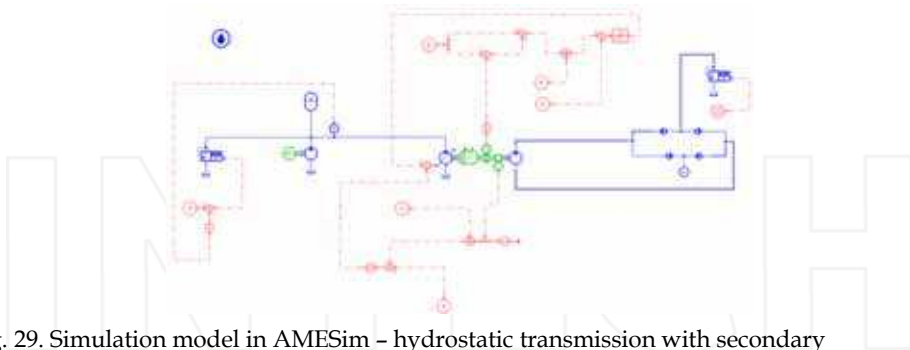


Fig. 29. Simulation model in AMESim – hydrostatic transmission with secondary adjustment: **variant (a)**

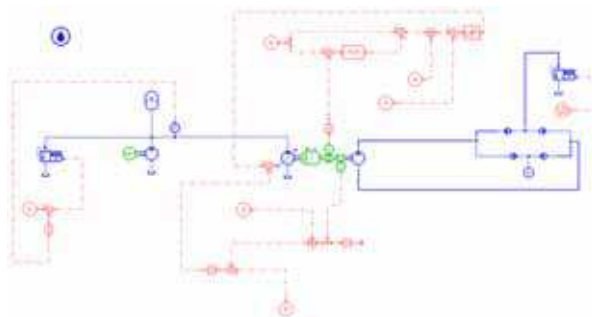


Fig. 30. Simulation model in AMESim – hydrostatic transmission with secondary adjustment: **variant (b)**

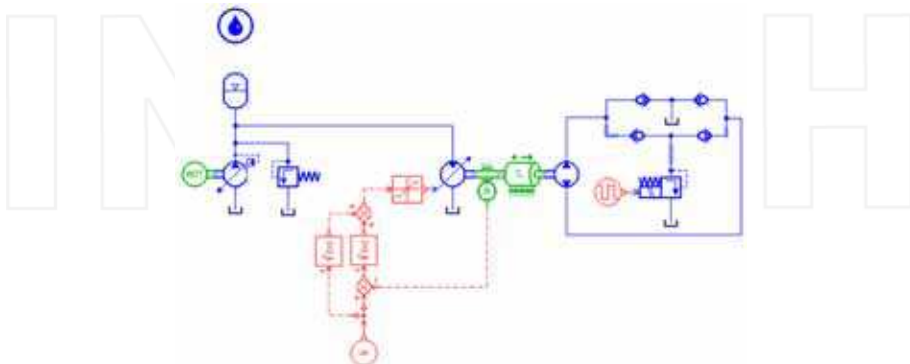


Fig. 31. Simulation model in AMESim – hydrostatic transmission with secondary adjustment: **variant (c)**

For the three simulation models the proportional pressure valve, associated with the fixed pump for simulation of the load of the servo motor within the secondary sector of hydrostatic transmission, is excited with a rectangular signal. We traced variation over time of the rotational speed of hydraulic servo motor, caused by variation of its load. Simulation model – variant (c) is run simultaneously for three maximum values of the capacity of hydraulic servo motor. Obtained results are presented in fig.32, fig.33 and fig.34.

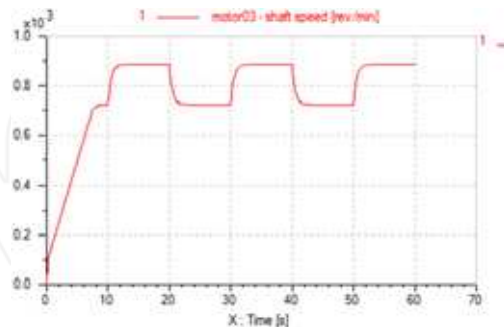


Fig. 32. Variation of rotational speed of hydraulic motor-variant (a)

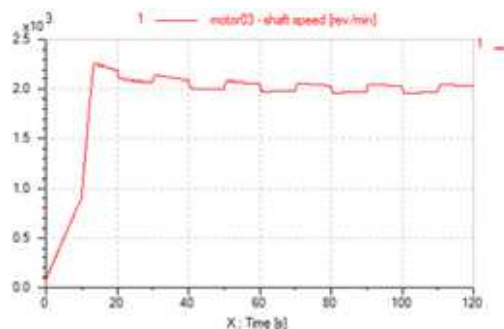


Fig. 33. Variation of rotational speed of hydraulic motor-variant (b)

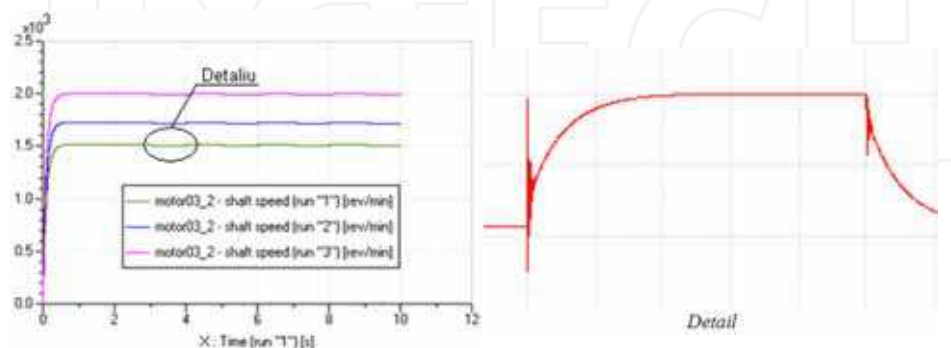


Fig. 34. Variation of rotational speed of hydraulic motor-variant (c)

4. Conclusions

Obtaining mathematical models, as close as possible to physical phenomena which are intended to be replicated or improved, help us in deciding how to optimize them. The introduction of computers in monitoring and controlling processes caused changes in technological systems. With support from the methods for identification of processes and from the power of numerical computing equipment, researchers and designers can shorten the period for development of applications in various fields by generating a solution as close as possible to reality, since the design stage.

4.1 Conclusions

As you can see from the diagrams of the transfer locus of servo mechanism (fig.7), its stability reserve increases along with decreasing amplification factor in flow of directional control valve around the null.

It can be noted that the amplification margin increases by about 15 percent when using directional control valve with variable area gradient, approaching the value 0.75, which is considered optimal in the literature (Vasiliu & Vasiliu, 2005).

Authors of this paper consider interesting the approach to simulate the method of enlarging the stability reserve by reducing the amplification factor around null and conditioning the control signal of distributing electromagnet to "trace" area profile of a slide valve "geometrically" shaped.

The advantages of using this method are: reduced cost of execution of slide valves, possibility to upgrade for systems without variable area gradient, improvement of performance of servo systems.

4.2 Conclusions

The adjustment model of a hydrostatic transmission, developed through technique of co-simulation AMESim/ LabVIEW, enables virtual and experimental analysis of phenomena specific to fluid power installations.

The web adjustment model of the hydrostatic transmission enables access to the drives and results of tests carried upon the physical laboratory model also for the persons outside the laboratory.

The adjustment model of a hydrostatic transmission with mixed adjustment enables remote control upon the parameters of hydraulic motor, depending on the actuation on hydraulic servomechanisms that adjust capacities of adjustable volumetric machines within the primary and secondary sectors.

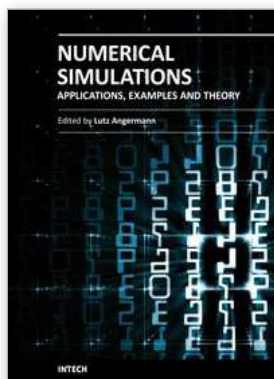
The developed adjustment model highlights the advantages in terms of energy of hydraulic transmissions with servopumps within their primary sector over transmissions with fixed pumps within their primary sector.

By means of successive simulations in AMESim, on three simulation models equivalent to the physic laboratory model, a hydraulic transmission with secondary adjustment was optimized, in terms of energy consumption and functional performances.

Optimal version of the simulation model, variant (c), represents the basis for optimization of the adjustment model for hydraulic transmissions with secondary adjustment, derived from the hydraulic transmission with mixed adjustment. In this variant of simulation the variation range of rotational speed of the hydraulic motor within the secondary sector, in conditions of variation of its load after a rectangular signal, is minimum, while through the pressure valve of the pump within the primary sector the extra flow is null.

5. References

- Bosch Rexroth Group - www.boschrexroth.com
- Calinoiu, C., Vasiliu, N. & Vasiliu, D. (1998). Modeling, Simulation and experimental Identification of the Hydraulic Servomechanisms, *Technical Publishing House*, Bucharest, Romania, 222 p., ISBN 973-31-1315-8
- Catana, I.; Vasiliu, D. & Vasiliu, N. (1996). Servomecanisme electrohidraulice, *Technical Publishing House*, POLITEHNICA University, Bucharest
- a. Drumea, P.; Popescu, T.C.; Blejan, M. & Rotaru, D. (2010). Research Activities Regarding Secondary and Primary Adjustment in Fluid Power Systems, *7th International Fluid Power Conference Aachen Efficiency through Fluid Power, Scientific Poster Session*, Aachen, Germany, 22-24 March 2010
- b. Drumea, P.; Popescu, T.C. & Ion Guta, D.D. (2010). Research activities regarding energetic and functional advantages of hydraulic transmissions, *Proceedings of SGEM 2010*, 10th International Multidisciplinary Scientific Geo-Conference & EXPO Modern Management of Mine Producing, Geology and Environmental Protection, Albena Resort-Bulgaria, 20 June - 25 June 2010
- a. Ion Guta, D.D.; Lepadatu, I.; Popescu, T.C. & Dumitrescu, C.(2010). Research on the stability of electrohydraulic servomechanisms developed with electrohydraulic amplifiers of variable area gradient, *Proceedings of 2010 International Conference on Optimisation of the Robots and Manipulators*, Calimanesti, Romania, 28-30 May, 2010
- b. Ion Guta, D.D.; Popescu, T.C. & Dumitrescu, C.(2010). Optimization of hydrostatic transmissions by means of virtual instrumentation technique, *Proceedings of ATOM-n 2010*, The 5th edition of the International Conference "Advanced Topics in Optoelectronics, Microelectronics and Nanotechnologies", 26-29 August 2010, Constanta, Romania
- LMS IMAGINE SA (2009). Advanced Modelling And Simulation Environment, Release 8.2.b., *User Manual*, Roanne, France
- National Instruments (2009). *User Manual*, NI USB-621x
- Popescu, T.C.; Ion Guta, D.D. & Marin, A. (2010). Adjustment of hydrostatic transmissions through virtual instrumentation technique, *ENERG_02, Proceedings of ISC 2010*, June 7-9, 2010, Budapest, Hungary
- Popescu, T.C.; Lepadatu, I. & Ion Guta, D.D. (2009). Experimental research activities regarding the reduction of energy compsumtion at endurance test stands of rotary volumetric machines, *Proceedings of International Scientific Technical Conference Hydraulics and Pneumatics 2009*, Wroclaw, 7-9 October, ISBN 978-83-87982-34-8, pp. 303-310.
- Vasiliu, N. & Vasiliu, D. (2005). Fluid Power Systems, Vol.I., *Technical Publishing House*, Bucharest, Romania, ISBN 973-31-2249-1



Numerical Simulations - Applications, Examples and Theory

Edited by Prof. Lutz Angermann

ISBN 978-953-307-440-5

Hard cover, 520 pages

Publisher InTech

Published online 30, January, 2011

Published in print edition January, 2011

This book will interest researchers, scientists, engineers and graduate students in many disciplines, who make use of mathematical modeling and computer simulation. Although it represents only a small sample of the research activity on numerical simulations, the book will certainly serve as a valuable tool for researchers interested in getting involved in this multidisciplinary field. It will be useful to encourage further experimental and theoretical researches in the above mentioned areas of numerical simulation.

How to reference

In order to correctly reference this scholarly work, feel free to copy and paste the following:

Teodor Costinel Popescu, Daniela Vasiliu and Nicolae Vasiliu (2011). Numerical Simulation - a Design Tool for Electro Hydraulic Servo Systems, Numerical Simulations - Applications, Examples and Theory, Prof. Lutz Angermann (Ed.), ISBN: 978-953-307-440-5, InTech, Available from:
<http://www.intechopen.com/books/numerical-simulations-applications-examples-and-theory/numerical-simulation-a-design-tool-for-electro-hydraulic-servo-systems>

INTeCH
open science | open minds

InTech Europe

University Campus STeP Ri
Slavka Krautzeka 83/A
51000 Rijeka, Croatia
Phone: +385 (51) 770 447
Fax: +385 (51) 686 166
www.intechopen.com

InTech China

Unit 405, Office Block, Hotel Equatorial Shanghai
No.65, Yan An Road (West), Shanghai, 200040, China
中国上海市延安西路65号上海国际贵都大饭店办公楼405单元
Phone: +86-21-62489820
Fax: +86-21-62489821